

Local Application of Isogenic Adipose-Derived Stem Cells Restores Bone Healing Capacity in a Type 2 Diabetes Model

CHRISTOPH WALLNER, STEPHANIE ABRAHAM, JOHANNES MAXIMILIAN WAGNER, KAMRAN HARATI, BRITTA ISMER, LUKAS KESSLER, HANNAH ZÖLLNER, MARCUS LEHNHARDT, BJÖRN BEHR

Key Words. Bone • Stem cells • Diabetes mellitus • Fractures • Osteogenesis

Department of Plastic Surgery, University Hospital Bergmannsheil, Ruhr University Bochum, Bochum, Germany

Correspondence: Björn Behr, M.D., Department of Plastic Surgery, BG University Hospital Bergmannsheil, Ruhr University Bochum, Bürkle-de-la-Camp-Platz 1, 44789 Bochum, Germany. Telephone: 49 234 3023443 or 49 234 3026379; E-Mail: bjorn.behr@rub.de

Received July 20, 2015; accepted for publication January 13, 2016.

©AlphaMed Press
1066-5099/2016/\$20.00/0

<http://dx.doi.org/10.5966/sctm.2015-0158>

ABSTRACT

Bone regeneration is typically a reliable process without scar formation. The endocrine disease type 2 diabetes prolongs and impairs this healing process. In a previous work, we showed that angiogenesis and osteogenesis—essential steps of bone regeneration—are deteriorated, accompanied by reduced proliferation in type 2 diabetic bone regeneration. The aim of the study was to improve these mechanisms by local application of adipose-derived stem cells (ASCs) and facilitate bone regeneration in impaired diabetic bone regeneration. The availability of ASCs in great numbers and the relative ease of harvest offers unique advantages over other mesenchymal stem cell entities. A previously described uncortical tibial defect model was utilized in diabetic mice (*Lepr^{db-/db-}*). Isogenic mouse adipose-derived stem cells (mASCs)^{db-/db-} were harvested, transfected with a green fluorescent protein vector, and isografted into tibial defects (150,000 living cells per defect). Alternatively, control groups were treated with Dulbecco's modified Eagle's medium or mASCs^{WT}. In addition, wild-type mice were identically treated. By means of immunohistochemistry, proteins specific for angiogenesis, cell proliferation, cell differentiation, and bone formation were analyzed at early (3 days) and late (7 days) stages of bone regeneration. Additionally, histomorphometry was performed to examine bone formation rate and remodeling. Histomorphometry revealed significantly increased bone formation in mASC^{db-/db-}-treated diabetic mice as compared with the respective control groups. Furthermore, locally applied mASCs^{db-/db-} significantly enhanced neovascularization and osteogenic differentiation. Moreover, bone remodeling was upregulated in stem cell treatment groups. Local application of mASCs can restore impaired diabetic bone regeneration and may represent a therapeutic option for the future. *STEM CELLS TRANSLATIONAL MEDICINE* 2016;5:1–9

SIGNIFICANCE

This study showed that stem cells obtained from fat pads of type 2 diabetic mice are capable of reconstituting impaired bone regeneration in type 2 diabetes. These multipotent stem cells promote both angiogenesis and osteogenesis in type 2 diabetic bony defects. These data might prove to have great clinical implications for bony defects in the ever-increasing type 2 diabetic patient population.

INTRODUCTION

Bony defects usually heal without scar formation. However, certain comorbidities delay and impair bone healing [1]. Diabetes mellitus was shown to markedly diminish fracture-healing capacity [2]. Most diabetic patients are suffering from type 2 diabetes (approximately 90%), with a predicted doubled prevalence worldwide for the year 2030 as compared with 2000 [3, 4]. In addition to an increased fracture risk in type 1 and 2 diabetes, fracture healing is detrimentally affected [5–8]. Loder showed that diabetic patients without neuropathy have a 1.6-fold delay in fracture healing [7]. Mechanisms causing increased fracture risk associated with paradox bone-density regulation,

delayed bone-healing capacity, higher prevalence for nonunions, and altered microarchitecture are poorly understood and the topic of current research [1, 5, 9]. Considering the epidemiological changes in combination with the severely altered bone metabolism, development of optimal treatment strategies for diabetes-associated diseases is in high demand.

So far, insights into mechanisms involved in diabetes-associated impairment of fracture healing were largely generated in type 1 diabetes mellitus (T1DM) animal models [10–12]. For instance, a distinct reduction of the proliferative capacity of the cell population of osteoprogenitor cells has been described in T1DM fractures in rats [10, 13, 14].

In addition, bone formation impairment was observed in a murine uncortical type 2 diabetes mellitus (T2DM) model [15]. Expression of the transcription factor Runt-related transcription factor 2 (RUNX-2), which is important for osteogenic differentiation, was markedly reduced in this model. Besides osteogenic differentiation, proliferating cell nuclear antigen (PCNA), which is indicative for cell proliferation, was significantly reduced in diabetic bony defects [15]. Thus, it is generally accepted that factors important for proliferation and differentiation in early and late bone healing are markedly altered in diabetic bony defects [14–16].

Angiogenesis is a crucial step in early bone regeneration and is decreased in T2DM defects [15, 17]. The importance of vascularization at the injury site is not only explained by the supply of nutrients, but also by migration of osteoprogenitors and other osteogenic cells [18]. Reduced expression of vascular endothelial growth factor (VEGF) was indicative for alterations in vascularization of T1DM animals [16]. Moreover, a current study showed that local application of VEGF distinctly increases angiogenesis and subsequently promotes bone healing in a T2DM model [15]. Additionally, implantation of adipose-derived stem cell (ASC)-derived endothelial cells improved vascularization of calvarial bone allografts [19]. The presence of ASCs induced neovascularization and osteocytic repopulation significantly [20]. Studies by Rehman et al. brought both concepts together by demonstrating that ASCs represent a source of VEGF [21]. Several studies have investigated the potential of ASC application in bony defects and reported significant improvements [22]. However, data of ASC application in diabetic bone regeneration are lacking. As such, wound-healing experiments in a T1DM animal model revealed a massive reduction of ASC recruitment and therefore impaired healing capacity [23].

We hypothesized that diminished bone regeneration in T2DM can be rescued by implantation of isogenic ASCs. Compared with bone marrow stromal cells, ASCs are much more abundant, are more accessible, and have lower donor morbidity, while showing similar capabilities in migration, differentiation, proliferation, and immunosuppression [22, 24, 25]. In our project, we conducted harvest and transfer of isogenic diabetic mouse adipose-derived stem cells (mASCs) to best mimic a potential clinical treatment approach.

MATERIALS AND METHODS

Isolation and Application of Mouse Adipose-Derived Stem Cells

Mouse adipose-derived stem cells were harvested from inguinal fat pads of db^{-}/db^{-} and wild-type (WT) mice and labeled similarly as previously described [17]. Briefly, inguinal fat pads were excised and washed in betadine/phosphate-buffered saline (PBS). Thereafter, fat pads were minced under sterile conditions and digested with 0.1% Collagenase A (Roche Diagnostics, Mannheim, Germany, <http://www.roche.com>) for 30 minutes at 37°C in a shaking water bath, centrifuged down, washed, and plated. Culture conditions were performed with Dulbecco's modified Eagle's medium (DMEM), GlutaMAX, 10% fetal bovine serum, 100 IU/ml penicillin, and 100 IU/ml streptomycin for in vitro experiments. mASCs were divided into four culture groups: cells from WT and diabetic animals in normal glucose (5.5 mM) and high glucose (22 mM) [26]. At passage 1 and 80% confluence, osteogenic

differentiation was initiated. Osteogenic differentiation medium (1% additional β -glycerolphosphate, 0.1% ascorbic acid; modified from Neuhuber et al. [27]) was changed every third day with glucose concentration accordingly. Cells were incubated at 37°C with a carbon dioxide level at 5%.

Alkaline phosphatase reaction (7 days after osteogenic differentiation) and Alizarin Red staining (28 days after osteogenic differentiation) were performed similarly as described [17]. In order to allow tracking of mASCs $^{db^{-}/db^{-}}$ in vivo, cells were labeled with a turboGFP lentiviral construct (GE Healthcare Life Sciences, Piscataway, NJ, <http://www.gelifesciences.com>). Briefly, mASCs $^{db^{-}/db^{-}}$ were treated with the construct and 8 μ g/ml polybrene at 80% confluence in a 10-cm dish. For 12 hours thereafter, cells were checked for green fluorescent protein (GFP) fluorescence and subsequently treated with puromycin to select only those cells transfected. For seeding purposes, mASCs $^{db^{-}/db^{-}}$ were trypsinized, washed with PBS, and counted.

Animal Surgery

All animal experiments were approved by the Institutional Animal Care and Use Committee, Landesamt für Natur, Umwelt und Verbraucherschutz Nordrhein-Westfalen. Heterozygous Lep^{db} (db^{+}/db^{-}) mice were obtained from the Jackson Laboratory (catalog no. 000697, Jackson Laboratory, Bar Harbor, ME, <https://www.jax.org>) and kept with unlimited access to water and standard laboratory chow. Heterozygous db^{+}/db^{-} mice on a C57BL/6J background were mated to obtain WT, db^{+}/db^{-} , and db^{-}/db^{-} mice. Genotyping for breeding was performed on genomic DNA by restriction enzyme digest after polymerase chain reaction (forward primer: ATGACCACTACAGATGAACCCAGTCTAC; reverse primer: CATTCAAACCATAGTTTGGTTGTC) according to Horvat and Büniger [28]. Female littermates at age 16–20 weeks were used for all experiments. All surgical procedures were performed under inhalation anesthesia with isoflurane and buprenorphine (Abbott GmbH, Wiesbaden, Germany, <http://www.abott.de>). An established murine tibial defect model was performed as previously described [29]. Briefly, after shaving and disinfecting the left leg, an incision was made on the proximal anterior skin surface over the tibia. After splitting the anterior tibial muscle, the tibia was properly exposed. A 1-mm uncortical defect was created on the anterior tibial surface. The six animal groups included (a) diabetic animals treated with 1.5×10^5 mASCs $^{db^{-}/db^{-}}$; (b) 1.5×10^5 mASCs WT in DMEM; (c) diabetic control animals treated with DMEM without cells; (d) WT animals treated with 1.5×10^5 mASCs $^{db^{-}/db^{-}}$; (e) 1.5×10^5 mASCs WT in DMEM; and (f) WT control animals with DMEM without cells. Lactic acid films were used as protective cover over the inserted medium, modified as previously described [30]. Wound closure was performed with 6-0 Prolene interrupted sutures. The anterior tibial muscle was reset into its anatomical position. Each group consisted of at least seven animals. Euthanasia was performed according to national and international laws and guidelines. Briefly, cervical dislocation was performed after thorough anesthesia to harvest tissue.

Tissue Preparation and Histological Procedures

Tibiae were harvested at a given time, fixed in 4% paraformaldehyde (Sigma-Aldrich, St. Louis, MO, <http://www.sigmaaldrich.com>) overnight at 4°C, and decalcified in 19% EDTA (PanReac AppliChem, Darmstadt, Germany, <https://www.applichem.com>) for 5 days with daily changes of solution. Samples were then

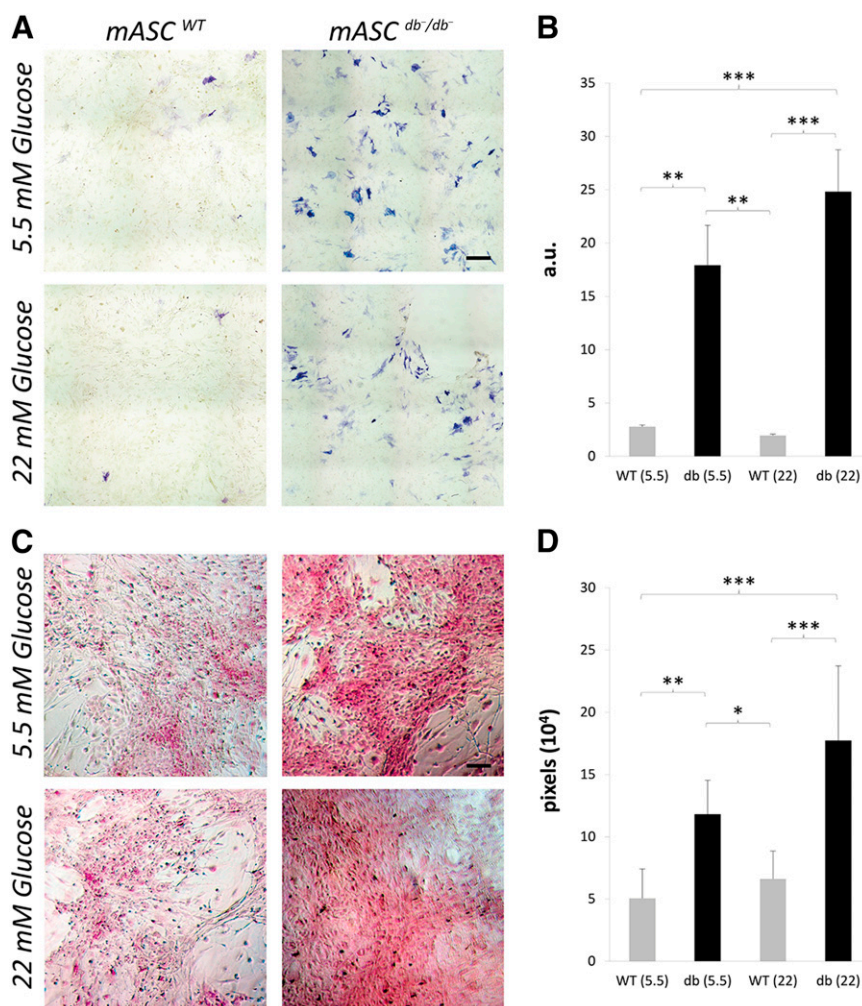


Figure 1. mASCs^{db/db} showed increased osteogenic differentiation as compared with mASCs^{WT}. **(A):** Alkaline phosphatase (ALP) activity on 7 days differentiated mASCs from diabetic and WT animals in both media (5.5 and 22 mM glucose). mASCs from diabetic origin showed increased activity. **(B):** Photometric measurement of ALP reaction. **(C):** Alizarin red staining of osteogenically differentiated mASCs in normoglycemic and hyperglycemic medium (5.5 and 22 mM glucose) showed increased mineralization as compared with mASCs^{WT} in both media. **(D):** Quantification of Alizarin red-positive pixels revealed highly significant increased mineralization rates of mASCs^{db/db} in both media compared with mASCs^{WT}. Results are shown as means \pm SEM. *, $p < .05$; **, $p < .01$; ***, $p < .001$ (two-sample *t* test). Scale bars = 10 μ m **(A)**, 15 μ m **(C)**. Abbreviations: a.u., arbitrary units; mASC, mouse adipose-derived stem cell; WT, wild type.

dehydrated, embedded in paraffin, and cut into serial sagittal sections (thickness 6–9 μ m).

For immunohistochemical stainings of RUNX-2 (rabbit, polyclonal; Santa Cruz Biotechnology, Santa Cruz, CA, <http://www.scbt.com>; sc-10758, 1:50, RUNX-2, AB_2184247), sections were incubated at 58°C for 1 hour and subsequently rehydrated and incubated with 0.125% Proteinase K for 30 minutes. After a short washing step with PBS, sections were permeabilized with 0.1% Tween 20 for 4 minutes and treated with blocking solution for 1 hour. Incubation with primary antibodies followed overnight in blocking solution at 4°C. After washing with PBS, a rabbit biotinylated secondary antibody followed by the AB reagent and NovaRED (Vector Laboratories, Burlingame, CA, <http://vectorlabs.com>) was used for detection. For PCNA detection, a PCNA Staining Kit (Thermo Fisher Scientific Life Sciences, Waltham, MA, <http://www.thermofisher.com>) was used according to manufacturer's protocols. Images were taken with an AxioImager M2 Imaging System (Zeiss, Stuttgart, Germany, <http://www.zeiss.com>).

For immunohistochemical staining of platelet endothelial cell adhesion molecule 1 (PECAM-1), vascular cell adhesion molecule 1 (VCAM-1) PCNA retrieval was performed by incubating rehydrated sections with 0.125% Proteinase K (Roche) in 10 mM Tris (pH 6.8) for 10 minutes at 37°C. Sections were blocked (10% normal goat serum (Vector Laboratories) and permeabilized with 0.1% Triton X-100 (Sigma-Aldrich) in PBS for 1 hour. Next, incubation with primary antibody specific for PECAM-1 (rat, monoclonal; catalog no. 553370, BD Biosciences, Heidelberg, Germany, <http://www.bdbiosciences.com>; 1:400, PECAM, AB_394816), VCAM-1 (rabbit, Santa Cruz Biotechnology, sc-1504, 1:50, V-CAM1), and PCNA (rabbit, Santa Cruz Biotechnology, sc-7907, 1:50, PCNA) was carried out overnight at 4°C. After washing with PBS, secondary antibody (goat anti-rat conjugated with Alexa 594, Thermo Fisher Scientific Life Sciences 1:1,000 dilution in PBS) has been applied and incubated for 4 hours at room temperature. All sections were counterstained with 4',6-diamidino-2-phenylindole (DAPI). Sections were subsequently mounted with

Fluoromount Aqueous Mounting Medium (Sigma-Aldrich). Images for immunofluorescence were taken with a fluorescence microscope (model IX83, Olympus, Tokyo, Japan, <http://www.olympus.co.jp>).

Quantification of Bone Formation

Every sixth section was used to characterize bone formation with aniline blue (Carl Roth, Karlsruhe, Germany, <https://www.carlroth.com>) staining as previously described [31]. Images were taken with a bright-field microscope (Zeiss Axiovert 100) and the following settings with Axiovision 4.8: objective $\times 2.5$, exposure time 614 ms, dimensions $3,900 \times 3,090$ pixels (Px), scanned color. Histomorphometric measurements of aniline blue-stained sections were performed in Adobe Photoshop (Adobe, San Jose, CA, <http://www.adobe.com>) with modifications [32]. Briefly, a $2,000 \times 2,000$ -Px dimensioned selection box was placed to cover the entire defect area. By using the Adobe Magic Wand Tool (settings: tolerance 60%; noncontiguous), new osteoid formation was selected semiautomatically. Tonal separation in two steps and deselecting existing cortical bone resulted in highlighted pixels reliably corresponding to bone formation area.

Assessment of Blood Vessel Sprouting

PECAM-1-positive endothelial cells and blood vessels were histomorphometrically quantified in a predefined area of $4,000 \times 4,000$ Px. Pixel count was fully automated in Adobe Photoshop by measuring PECAM-1-positive pixel, subtracting background staining from control. This corresponded to the PECAM-1-positive endothelial cells. Blood vessel sprouting was analyzed on at least four stained slides per defect by two blinded independent examiners.

Differentiation and Proliferation Analysis

Analogous to quantification of bone formation, a region of interest was selected ($2,000 \times 2,000$ Px). Immunohistochemically, RUNX-2- and PCNA-positive stained pixels were automatically selected by using the Adobe Magic Wand Tool (settings: tolerance 60%; noncontiguous).

The analysis of spatial proximity of RUNX-2, PCNA, and PECAM staining (red) in relation to GFP-positive pixels (green) was performed by setting a numerical relationship. Merged pixels (GFP-positive pixels and target-specific pixels [RUNX-2, PCNA, and PECAM], yellow) were placed into proportion to target specific pixels (red) to calculate the ratio of autocrine cells versus paracrine-stimulated cells.

Statistics

Results of the study are presented as mean \pm SEM of at least three independent experiments. *p* values were calculated by Student's *t* test comparing two groups and analysis of variance if comparing more than two groups. Statistical significances were set at *p* < .05.

RESULTS

mASCs^{db-/db-} Showed Increased Osteogenic Potential as Compared with mASCs^{WT} In Vitro

First, we analyzed the osteogenic potential of mASCs^{db-/db-} and mASCs^{WT} in vitro (Fig. 1). In order to study an intermediate stage

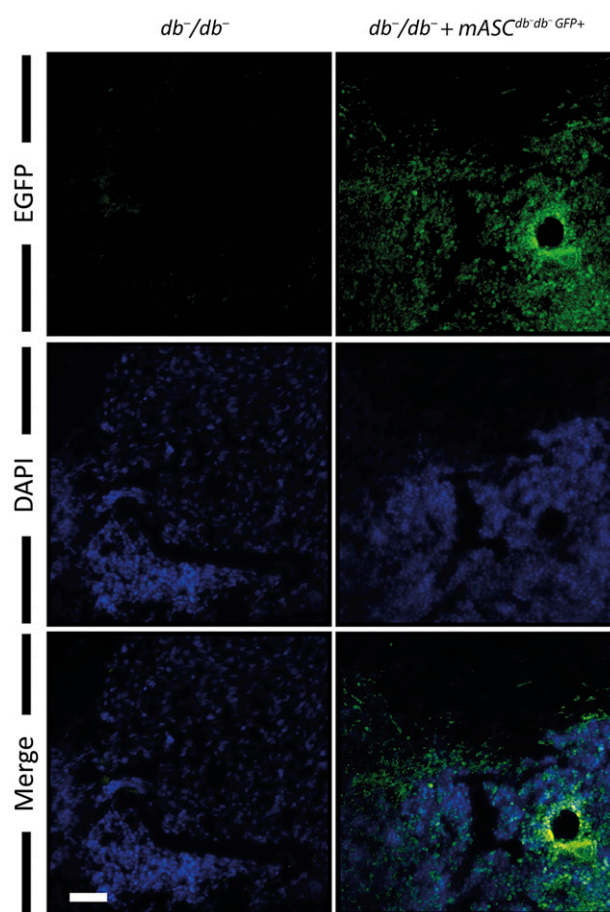


Figure 2. Successful colonization of mASCs^{db-/db-GFP+} in diabetic defects. Defects were colonized with isogenic GFP-positive (green) mASCs^{db-/db-} (1.5×10^5 mASCs^{db-/db-}; right column). GFP-positive cells indicate successful colonization (left column; comparison with diabetic defect without treatment). Scale bar = 20 μ m. Abbreviations: DAPI, 4',6-diamidino-2-phenylindole; EGFP, enhanced green fluorescent protein; GFP, green fluorescent protein; mASC, mouse adipose-derived stem cell.

of osteogenic differentiation, enzymatic alkaline phosphatase (ALP) assay was performed at 7 days differentiation. Interestingly, mASCs^{db-/db-} showed a significantly increased ALP activity as compared with mASCs^{WT} in both normoglycemic and hyperglycemic conditions. We next analyzed a late stage of osteogenesis by performing Alizarin red staining to determine calcification of extracellular matrix at day 28 of osteogenic differentiation [17]. Histomorphometry revealed increased mineralization of mASCs^{db-/db-} in both hyperglycemic and normoglycemic media, as compared with mASCs^{WT} (Fig. 1).

mASCs^{db-/db-} in Bony Defects

Next, we sought to evaluate the osteogenic potential of mASCs^{db-/db-} in vivo. In order to ensure proper colonization of mASCs^{db-/db-GFP+} at the injury site and validate the seeding procedure, fluorescence microscopy pictures for enhanced green fluorescent protein (EGFP) and DAPI were taken 7 days postoperation (dpo) comparing diabetic defects seeded with transplanted mASCs^{db-/db-} with the control group (DMEM only). Indeed, immunofluorescence verified successful colonization of defects treated with transplanted mASCs^{db-/db-} (Fig. 2).

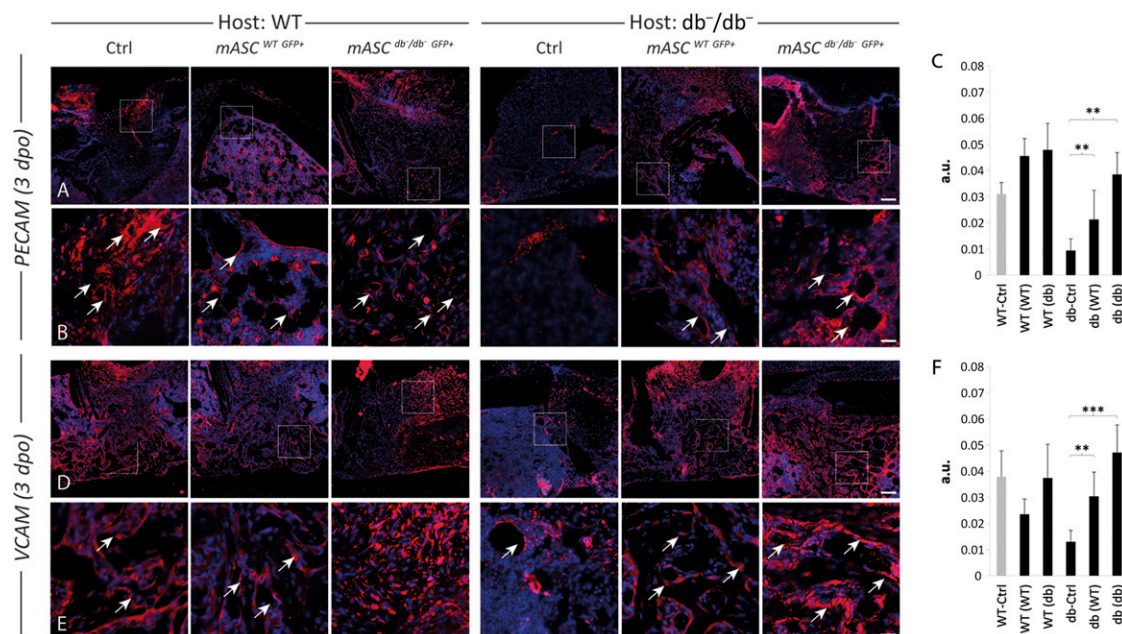


Figure 3. Isogenic mASCs^{db/db} and mASC^{WT} increase angiogenesis in diabetic defects. **(A):** Blood vessels and endothelial cells were detected by immunofluorescence for PECAM-1 (3 dpo). db⁻/db⁻ control mice exhibited decreased angiogenesis compared with control WT mice (left column), whereas defects treated with mASCs^{db/db} (right column) showed a significant improvement in angiogenesis compared with control animals without treatment (db-Ctrl). Although all mASC-transplanted mice exhibited improved angiogenesis, mASCs^{db/db} did show the highest increase in angiogenesis. **(B):** Higher magnifications from **(A)** (white box). **(C):** Quantification of PECAM-1-positive pixels (arbitrary units) revealed that angiogenesis is significantly increased in mASCs-treated defects compared with diabetic defects without treatment and rescued to levels of WT control mice. mASCs transplanted into WT mice have shown a further improvement to WT-control animals. **(D):** Blood vessels and endothelial cells were detected by immunofluorescence for VCAM-1 (3 dpo). Results largely paralleled PECAM-1 staining. **(E):** Higher magnifications from **(D)** (white box). **(F):** Quantification of VCAM-1-positive pixels (arbitrary units) revealed that angiogenesis is significantly increased in mASC-treated defects compared with diabetic defects without treatment and rescued to levels of WT mice. Results are shown as means \pm SEM. **, $p < .01$; ***, $p < .001$ (two-sample t test). Scale bars = 200 μ m (**A, D**), 20 μ m (**B, E**). Abbreviations: a.u., arbitrary units; Ctrl, control; dpo, days postoperation; GFP, green fluorescent protein; mASC, mouse adipose-derived stem cell; PECAM-1, platelet endothelial cell adhesion molecule 1; VCAM-1, vascular cell adhesion molecule 1; WT, wild type.

Angiogenesis Is Increased by Local Application of mASCs

Angiogenesis is a crucial step in bone regeneration. In order to investigate the effects of mASCs on angiogenesis in diabetic bone regeneration, immunohistochemical stainings for PECAM-1 were performed. Immunohistochemistry revealed a significant increase in endothelial cell count in diabetic bone regeneration after local application of isogenic (db⁻/db⁻ origin) and allogenic (WT origin) mASCs compared with diabetic control animals 3 dpo. mASCs^{db/db} treated diabetic mice showed similar PECAM-1 levels as WT controls. We did not see significant improvement of angiogenesis in mASC-implanted WT mice compared with WT control animals. These findings were confirmed by immunohistochemistry for VCAM-1 (Fig. 3).

Local Application of mASCs Enhanced Osteogenic Differentiation and Proliferation

To further evaluate the capability of mASCs to stimulate local osteogenic differentiation and proliferation, immunohistochemistry for PCNA (proliferation) and RUNX-2 (osteogenic differentiation) was carried out at 3 dpo. Moreover, we performed immunohistochemistry for osteocalcin, a late marker for osteogenesis at 7 dpo. Our findings confirmed that, after local application of mASCs, osteogenesis, proliferation, and terminal differentiation were significantly enhanced in mASC^{db/db}-treated diabetic mice compared with diabetic control mice. This group

reached PCNA, RUNX-2, and osteocalcin levels similar to the WT control group. Local treatment of bony defects with mASCs^{WT} in WT animals showed no significant increases of PCNA, RUNX-2, or osteocalcin expression compared with WT control animals (Fig. 4).

Osteogenesis Is Markedly Increased in Late Bone Regeneration After Isogenic mASC^{db/db} Transplantation

In order to analyze bone formation after application of mASCs, we performed aniline blue staining to detect osteoid formation 7 dpo. Aniline blue staining revealed a significant increase of bone regeneration in diabetic animals treated by local administration of mASCs^{db/db}, mimicking physiological bone regeneration in WT control mice (Fig. 5). We did not observe significant improvement of osteogenesis in WT animals transplanted with mASCs^{db/db} or mASCs^{WT}.

Paracrine Effects Dominate Increases in Angiogenic and Osteogenic Differentiation Mediated by mASCs^{db/db}

We analyzed the spatial proximity of transplanted mASCs^{db/db} and indicators of proliferation, angiogenesis, and osteogenic differentiation to evaluate paracrine and cell-autonomous effects. We performed immunofluorescence staining to estimate functions of the transplanted mASCs. In all three groups,

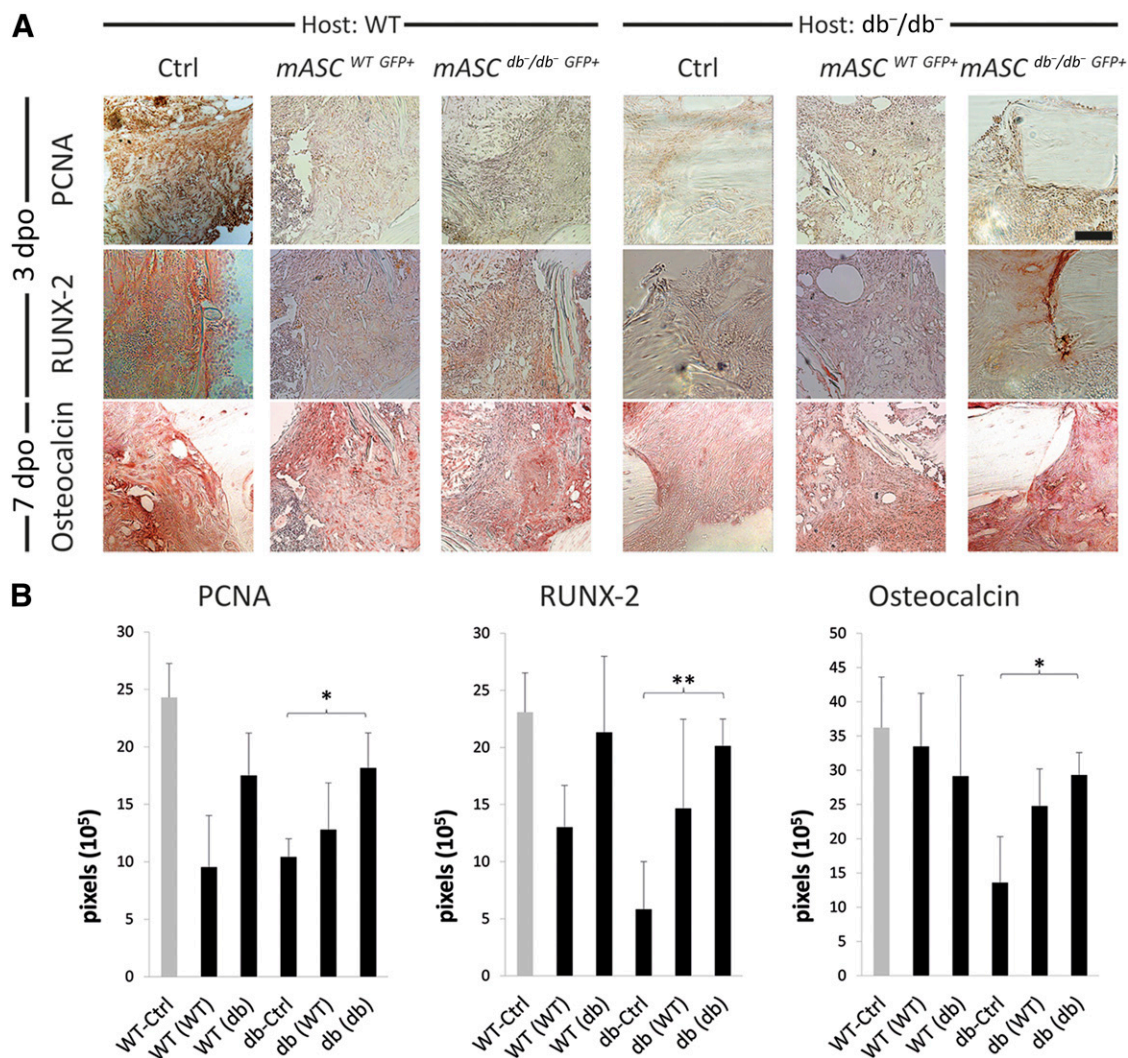


Figure 4. mASCs^{db⁻/db⁻} application enhances proliferation and differentiation in diabetic bony defects. **(A)**: Immunohistochemistry for PCNA, RUNX-2, and osteocalcin revealed enhancement of osteogenic and proliferative capacity in mASCs^{db⁻/db⁻}-treated diabetic animals compared with control group (db⁻/db⁻). **(B)**: Quantification of Nova Red-positive pixels showed that cell proliferation and differentiation are significantly increased in diabetic animals treated with mASCs^{db⁻/db⁻} compared with untreated animals. Application of mASCs^{WT} into diabetic defects showed no significant improvement in PCNA, RUNX-2, or osteocalcin expression. WT defects treated with mASCs showed no significant alteration in PCNA, RUNX-2, or osteocalcin expression. Results are shown as means ± SEM. *, $p < .05$; **, $p < .01$ (two-sample t test). Scale bar = 200 μ m. Abbreviations: Ctrl, control; dpo, days postoperation; mASC, mouse adipose-derived stem cell; PCNA, proliferating cell nuclear antigen; RUNX-2, Runt-related transcription factor 2; WT, wild type.

we detected both cell-autonomous and paracrine effects, with a ratio favoring paracrine effects in PECAM (1:2.8) and RUNX-2 (1:5.9) stainings. In contrast, both effects were accountable in PCNA stainings (1:1.1) (Fig. 6).

DISCUSSION

In this study, we investigated the effects of isogenic mASCs^{db⁻/db⁻} in type 2 diabetic bone regeneration and explored their osteogenic and angiogenic potential. We could demonstrate that transplanted mASCs^{db⁻/db⁻} were capable of successful colonization inside the bony defect. Moreover, our experiments revealed that local application of mASCs^{db⁻/db⁻} completely rescued bone regeneration in diabetic defects accompanied by significant enhancement of angiogenesis, proliferation (PCNA), osteogenic differentiation (RUNX-2), and expression of osteocalcin.

Most diabetes-related bone studies are conducted in T1DM animal models. Particularly with regard to angiogenesis, a T2DM model associated with a metabolic syndrome is highly demanded. In previous work, angiogenesis has been shown to be reduced in T2DM bone regeneration, due to impaired recruitment of endothelial progenitor cells and endothelial cell migration [15]. In our experiments, mASCs^{db⁻/db⁻} were capable of promoting angiogenesis in the bony defect zone in db⁻/db⁻ mice compared with the control group.

Besides angiogenesis, cell proliferation constitutes an integral part of fracture healing. PCNA, a protein synthesized during cell replication, is upregulated in the bony defect zone of the mASC^{db⁻/db⁻} transplanted db⁻/db⁻ mice. Combination of RUNX-2 and PCNA is indicative for differentiation of osteoprogenitor cells [15]. Enhanced levels of RUNX-2 and PCNA are consistent with increased osteocalcin level in mASC^{db⁻/db⁻}

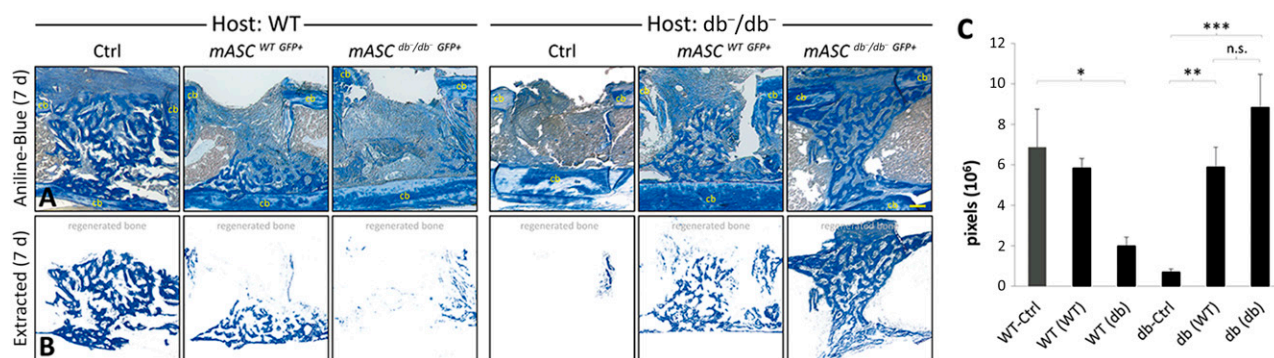


Figure 5. mASCs^{db⁻/db⁻} increase bone regeneration in diabetic bony defects. **(A):** Aniline blue staining of db⁻/db⁻ control mice showed impaired new bone formation compared with WT control mice (left column), whereas diabetic defects treated with mASCs^{db⁻/db⁻} showed improved bone formation (right column) (7 dpo). Transplantation of mASCs^{db⁻/db⁻} and mASCs^{WT} into WT mice did not improve bone formation. **(B):** Extracted osteoid formation area. **(C):** Quantification of aniline blue-positive pixels revealed that bone formation is significantly increased in mASC-treated diabetic defects compared with the control group db⁻/db⁻ and similar to bone formation of WT mice. mASC implantation into WT mice did not show improved bone regeneration. Results are shown as means ± SEM. Scale bar = 200 μm. *, *p* < .05; **, *p* < .01; ***, *p* < .001 (two-sample *t* test). Abbreviations: Cb, cortical bone; Ctrl, control; d, days postoperation; mASC, mouse adipose-derived stem cell; n.s., not significant; WT, wild type.

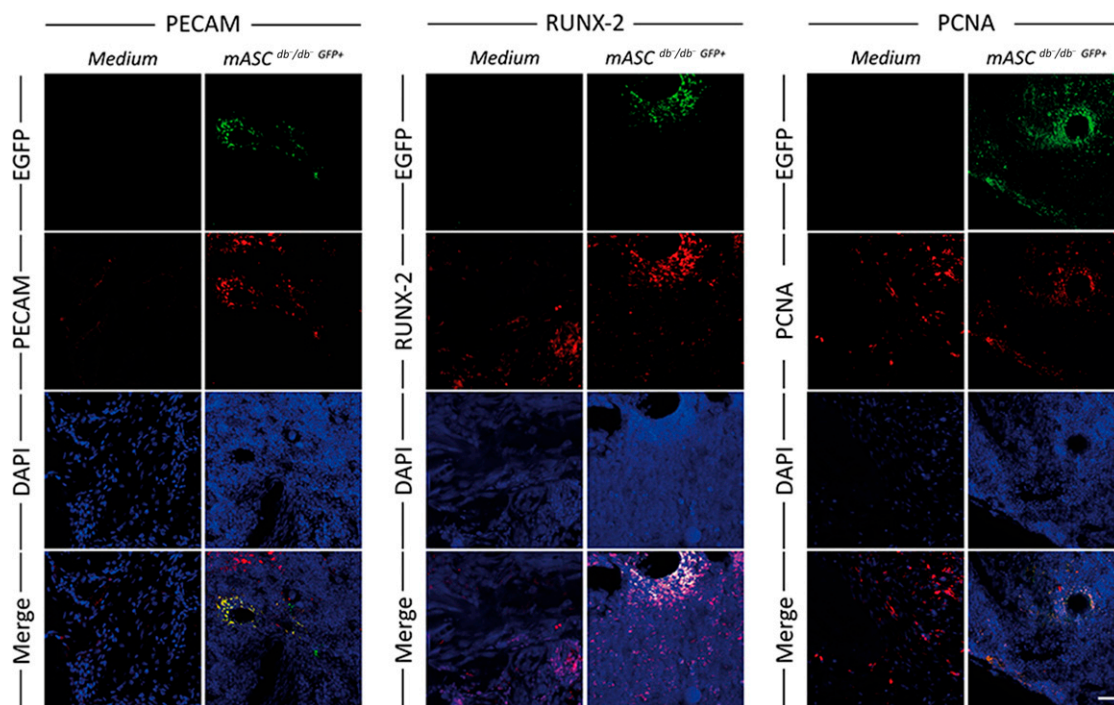


Figure 6. Paracrine effects dominate increases in angiogenic and osteogenic differentiation mediated by mASCs^{db⁻/db⁻-GFP⁺}. Immunofluorescence stainings were performed for PECAM, RUNX-2, and PCNA in diabetic mice transplanted with mASC^{db⁻/db⁻-GFP⁺} and controls. EGFP-positive areas indicate transplanted stem cells. Scale bar = 40 μm. Abbreviations: DAPI, 4',6-diamidino-2-phenylindole; EGFP, enhanced green fluorescent protein; GFP, green fluorescent protein; mASC, mouse adipose-derived stem cell; PCNA, proliferating cell nuclear antigen; PECAM, platelet endothelial cell adhesion molecule; RUNX-2, Runt-related transcription factor 2.

transplanted db⁻/db⁻ mice and depicts improved bone regeneration.

In diabetes, the puzzling situation of a pro-osteogenic hyperinsulinemia with concurrent antiosteogenic hyperglycemia occurs [33]. Experiments have shown that chronic hyperglycemia decreases the osteogenic and angiogenic potential of osteoprogenitors [34]. Similar results were obtained in another study, suggesting the osmolar activity of glucose as a component of impaired osteoblast maturation [34]. Additionally, hyperglycemia leads to a decreased expression of RUNX-2 and therefore

diminishes osteogenesis in favor of adipogenesis [35]. Taken together, antiosteogenic effects outweigh in the hyperglycemic condition in vivo.

In contrast, it has been shown that the hyperglycemic condition elevates the proliferative and differentiative capacity of adipocyte-derived stem cells in vitro [36]. We were able to show increased mineralization and differentiation of mASCs^{db⁻/db⁻} in vitro in both normoglycemic and hyperglycemic media as compared with mASCs^{WT}. However, it is difficult to reproduce the complex interplay of all in vivo factors in an in vitro setting.

Concluding, isolated chronic hyperglycemia of stem cells of diabetic origin enhances the osteogenic stem cell differentiation in vitro [37], whereas diabetes-related compromised angiogenesis, inflammatory environment, and chronic hyperglycemia reduce osteogenic potential in vivo. In our current study, mASCs^{db-/db-} surpass the osteogenic potential of mASCs^{WT} in both normoglycemic and hyperglycemic conditions in vitro. The chronically deviated expression patterns of mASCs^{db-/db-} in their original milieu might cause their higher osteogenic potential in vitro, omitting the compromising systemic adverse effects of diabetes in vivo [2, 34, 36, 37].

Moreover, we wanted to address the question of whether transplanted mASCs^{db-/db-GFP+} elicit paracrine or cell-autonomous effects. Our findings emphasize that mASCs^{db-/db-GFP+} largely have a paracrine and, to a lesser degree, cell-autonomous effect on differentiation and angiogenesis congruent with previous studies [17, 38]. The high proliferative activity of the mASCs implied the largely cell-autonomous effect on proliferation.

The impact of diabetes mellitus on mASCs remains a topic of current scientific discussion. BMP-4, a protein involved in the maintenance of stem cells, is elevated in diabetes mellitus; concordantly, the BMP-4 inhibitor matrix Gla protein is decreased [39]. Multiple endothelial cell markers are increased in inguinal fat pads of diabetic rats, indicating an amplified vascularity. Diabetic dedifferentiated fat cells exhibit an enhancement of both endothelial and adipogenic lineage differentiation [39]. Our findings in application of mASCs^{db-/db-} from diabetic animals resemble these findings, indicating that stem cell lineages from diabetic animals have a higher osteogenic differentiation potential in vitro.

Given the relatively simple methods to lipoaspirate tissue containing ASCs and differentiate the harvested cells into the bone lineage in vivo, an established routine of aesthetic surgery may be modified [40, 41]. Today, aesthetic surgical practice is unselective transfer of lipoaspirates. The innovative therapeutic concept would be a lipoaspiration of human fat tissue, purification of ASCs, subsequent differentiation, and autotransplantation in diabetic patients with bony defects analogous to the implementation in this study. Current obstacles are the poor osmotic nutrition and the necessity of neovascularization of the

transferred cells, which might be addressed by supply of angiogenic factors [42, 43].

CONCLUSION

In the current study, we have demonstrated that isogenic transplantation of mASCs^{db-/db-} enhanced both osteogenesis and angiogenesis in diabetic bone regeneration. Proteins specific for osteogenic and angiogenic activity as well as mineralization and osteoid formation were elevated in diabetic bone defects treated with mASCs^{db-/db-} and quantitatively reversed to physiological bone healing in WT animals. This study can serve as a basis for future translational studies performed in large animals and humans to overcome the epidemiological and economical hurdles of diabetic bony injuries.

ACKNOWLEDGMENTS

This work was supported by German Research Foundation Grant DFG BE 4169/3-1 (to B.B.).

AUTHOR CONTRIBUTIONS

C.W.: administrative support, conception and design, provision of study material or patients, collection and/or assembly of data, data analysis and interpretation, manuscript writing, final approval of manuscript; S.A.: administrative support, provision of study material or patients, collection and/or assembly of data, data analysis and interpretation; J.M.W., K.H., B.I., L.K., and H.Z.: provision of study material or patients, collection and/or assembly of data, final approval of manuscript; M.L.: administrative support, conception and design, financial support, manuscript writing, final approval of manuscript; B.B.: administrative support, conception and design, financial support, provision of study material or patients, collection and/or assembly of data, data analysis and interpretation, manuscript writing, final approval of manuscript.

DISCLOSURE OF POTENTIAL CONFLICTS OF INTEREST

The authors indicated no financial relationships.

REFERENCES

- Gaston MS, Simpson AHRW. Inhibition of fracture healing. *J Bone Joint Surg Br* 2007;89-B:1553–1560.
- Retzepi M, Donos N. The effect of diabetes mellitus on osseous healing. *Clin Oral Implants Res* 2010;21:673–681.
- Daneman D. Type 1 diabetes. *Lancet* 2006;367:847–858.
- Wild S, Roglic G, Green A et al. Global prevalence of diabetes: eEstimates for the year 2000 and projections for 2030. *Diabetes Care* 2004;27:1047–1053.
- Isidro ML, Ruano B. Bone disease in diabetes. *Curr Diabetes Rev* 2010;6:144–155.
- Khazai NB, Beck GR Jr., Umpierrez GE. Diabetes and fractures: An overshadowed association. *Curr Opin Endocrinol Diabetes Obes* 2009;16:435–445.
- Loder RT. The influence of diabetes mellitus on the healing of closed fractures. *Clin Orthop Relat Res* 1988;232:210–216.
- Cozen L. Does diabetes delay fracture healing? *Clin Orthop Relat Res* 1972;82:134–140.
- Schwartz AV. Diabetes mellitus: Does it affect bone? *Calcif Tissue Int* 2003;73:515–519.
- Beam HA, Parsons JR, Lin SS. The effects of blood glucose control upon fracture healing in the BB Wistar rat with diabetes mellitus. *J Orthop Res* 2002;20:1210–1216.
- Fowlkes JL, Bunn RC, Liu L et al. Runt-related transcription factor 2 (RUNX2) and RUNX2-related osteogenic genes are down-regulated throughout osteogenesis in type 1 diabetes mellitus. *Endocrinology* 2008;149:1697–1704.
- Botolin S, Faugere M-C, Malluche H et al. Increased bone adiposity and peroxisomal proliferator-activated receptor-gamma2 expression in type I diabetic mice. *Endocrinology* 2005;146:3622–3631.
- Gebauer GP, Lin SS, Beam HA et al. Low-intensity pulsed ultrasound increases the fracture callus strength in diabetic BB Wistar rats but does not affect cellular proliferation. *J Orthop Res* 2002;20:587–592.
- Tyndall WA, Beam HA, Zarro C et al. Decreased platelet derived growth factor expression during fracture healing in diabetic animals. *Clin Orthop Relat Res* 2003;408:319–330.
- Wallner C, Schira J, Wagner JM et al. Application of VEGFA and FGF-9 enhances angiogenesis, osteogenesis and bone remodeling in type 2 diabetic long bone regeneration. *PLoS One* 2015;10:e0118823.
- Gandhi A, Doumas C, O'Connor JP et al. The effects of local platelet rich plasma delivery on diabetic fracture healing. *Bone* 2006;38:540–546.
- Behr B, Tang C, Germann G et al. Locally applied vascular endothelial growth factor A increases the osteogenic healing capacity of human adipose-derived stem cells by promoting osteogenic and endothelial differentiation. *STEM CELLS* 2011;29:286–296.
- Glowacki J. Angiogenesis in fracture repair. *Clin Orthop Relat Res* 1998(355 suppl):S82–S89. doi:10.1097/00003086-199810001-00010

- 19** Cornejo A, Sahar DE, Stephenson SM et al. Effect of adipose tissue-derived osteogenic and endothelial cells on bone allograft osteogenesis and vascularization in critical-sized calvarial defects. *Tissue Eng Part A* 2012;18:1552–1561.
- 20** Kloeters O, Berger I, Ryssel H et al. Revitalization of cortical bone allograft by application of vascularized scaffolds seeded with osteogenic induced adipose tissue derived stem cells in a rabbit model. *Arch Orthop Trauma Surg* 2011;131:1459–1466.
- 21** Rehman J, Traktuev D, Li J et al. Secretion of angiogenic and antiapoptotic factors by human adipose stromal cells. *Circulation* 2004;109:1292–1298.
- 22** Zuk P. Adipose-derived stem cells in tissue regeneration: A review. *ISRN Stem Cells* 2013;2013:713959.
- 23** Cianfarani F, Toietta G, Di Rocco G et al. Diabetes impairs adipose tissue-derived stem cell function and efficiency in promoting wound healing. *Wound Repair Regen* 2013;21:545–553.
- 24** Monaco E, Bionaz M, Hollister SJ et al. Strategies for regeneration of the bone using porcine adult adipose-derived mesenchymal stem cells. *Theriogenology* 2011;75:1381–1399.
- 25** Behr B, Ko SH, Wong VW et al. Stem cells. *Plast Reconstr Surg* 2010;126:1163–1171.
- 26** Zhang L, Li K, Liu X et al. Repeated systemic administration of human adipose-derived stem cells attenuates overt diabetic nephropathy in rats. *Stem Cells Dev* 2013;22:3074–3086.
- 27** Neuhuber B, Gallo G, Howard L et al. Reevaluation of in vitro differentiation protocols for bone marrow stromal cells: Disruption of actin cytoskeleton induces rapid morphological changes and mimics neuronal phenotype. *J Neurosci Res* 2004;77:192–204.
- 28** Horvat S, Bünger L. Polymerase chain reaction-restriction fragment length polymorphism (PCR-RFLP) assay for the mouse leptin receptor (*Lepr*(db)) mutation. *Lab Anim* 1999;33:380–384.
- 29** Behr B, Sorkin M, Manu A et al. Fgf-18 is required for osteogenesis but not angiogenesis during long bone repair. *Tissue Eng Part A* 2011;17:2061–2069.
- 30** James AW, Leucht P, Levi B et al. Sonic Hedgehog influences the balance of osteogenesis and adipogenesis in mouse adipose-derived stromal cells. *Tissue Eng Part A* 2010;16:2605–2616.
- 31** Rális ZA, Rális HM. A simple method for demonstration of osteoid in paraffin sections. *Med Lab Technol* 1975;32:203–213.
- 32** Behr B, Leucht P, Longaker MT et al. Fgf-9 is required for angiogenesis and osteogenesis in long bone repair. *Proc Natl Acad Sci USA* 2010;107:11853–11858.
- 33** Ferron M, Wei J, Yoshizawa T et al. Insulin signaling in osteoblasts integrates bone remodeling and energy metabolism. *Cell* 2010;142:296–308.
- 34** Botolin S, McCabe LR. Chronic hyperglycemia modulates osteoblast gene expression through osmotic and non-osmotic pathways. *J Cell Biochem* 2006;99:411–424.
- 35** Wang A, Midura RJ, Vasanji A et al. Hyperglycemia diverts dividing osteoblastic precursor cells to an adipogenic pathway and induces synthesis of a hyaluronan matrix that is adhesive for monocytes. *J Biol Chem* 2014;289:11410–11420.
- 36** García-Jiménez C, García-Martínez JM, Chocarro-Calvo A et al. A new link between diabetes and cancer: Enhanced WNT/ β -catenin signaling by high glucose. *J Mol Endocrinol* 2014;52:R51–R66.
- 37** Lopez R, Arumugam A, Joseph R et al. Hyperglycemia enhances the proliferation of non-tumorigenic and malignant mammary epithelial cells through increased leptin/IGF1R signaling and activation of AKT/mTOR. *PLoS One* 2013;8:e79708.
- 38** Caplan AI, Dennis JE. Mesenchymal stem cells as trophic mediators. *J Cell Biochem* 2006;98:1076–1084.
- 39** Jumabay M, Moon JH, Yeerna H et al. Effect of diabetes mellitus on adipocyte-derived stem cells in rat. *J Cell Physiol* 2015;230:2821–2828.
- 40** Moore JH Jr., Kolaczynski JW, Morales LM et al. Viability of fat obtained by syringe suction lipectomy: Effects of local anesthesia with lidocaine. *Aesthetic Plast Surg* 1995;19:335–339.
- 41** Halvorsen YD, Franklin D, Bond AL et al. Extracellular matrix mineralization and osteoblast gene expression by human adipose tissue-derived stromal cells. *Tissue Eng* 2001;7:729–741.
- 42** Ennett AB, Mooney DJ. Tissue engineering strategies for in vivo neovascularisation. *Expert Opin Biol Ther* 2002;2:805–818.
- 43** Gimble J, Guilak F. Adipose-derived adult stem cells: Isolation, characterization, and differentiation potential. *Cytherapy* 2003;5:362–369.